

PETROGRAPHY AND GEOCHEMISTRY OF MAFIC GRANULITES OF THE UBENDIAN BELT: CONTRIBUTION TO INSIGHTS INTO THE LOWER CONTINENTAL CRUST OF THE PALEOPROTEROZOIC

N Boniface

University of Dar es Salaam, College of Natural and Applied Sciences,
Department of Geology, P. O. Box 35052, Dar es Salaam, Tanzania

Email: nelson.boniface@udsm.ac.tz

ABSTRACT

Mafic granulites of the Ubendian Belt have geochemical signature, trace and REE patterns, similar to that of the lower continental crustal rocks. A SHRIMP U-Pb single zircon date at 1977 ± 40 Ma indicates that these rocks belong to the Paleoproterozoic Ubendian orogenic cycle, which was followed by the Mesoproterozoic tectonic disturbance that contributed to their exhumation. Orthopyroxene, clinopyroxene, garnet, hornblende, plagioclase and quartz is a frequent mineral assemblage for the mafic granulites of the Ubendian Belt, and garnet frequently form corona between plagioclase and clinopyroxene. Geothermobarometric calculations have revealed the equilibration of these rocks at a temperature range between 650 and 740 °C and pressure between 7 and 10.2 kbar equivalent to the geothermogradient of 22-28 °C/km and a depth of 23-33 km. Garnet coronas between plagioclase and clinopyroxene suggest a typical isobaric cooling P-T path for granulite terranes. The absence of preserved earlier (prograde) mineral assemblage suggests deep burial for these granulites, more than 33 km, and long stay for re-equilibration at relatively shallower crustal levels at 23-33 km deep.

Keywords: mafic granulite, isobaric cooling, zircon, Ubendian Belt

INTRODUCTION

Granulite-facies terranes are of particular interest to petrologists because granulites provide a window into the chemistry and *P-T* history of the lower crust (Spear 1993). Lower crust granulite terranes are characterized by near-isobaric cooling *P-T* paths, which manifest thermal relaxation and long residence times at the base of a crust of normal thickness. Near-isobaric cooling *P-T* paths could communicate a process of magmatic underplating or doubly thickened crust during orogeny (Ellis 1987). To uncover a complete shape of the *P-T* path, clockwise or ant-clockwise, in granulite terranes depend on the preservation of prograde mineral assemblages.

In recent years, analysis of the composition of the continental crust has gained more focus from geochemists. This is because large proportions of incompatible elements (20-70%) are contained in the continental

crust, despite its small volume and mass of only about 0.6% of the silicate Earth. Therefore the crust is the Earth's major repository of incompatible elements and thus factors prominently into geochemical mass balance calculations for the whole Earth (Rudnick and Gao 2003).

The aims of this study are: (1) to time the mafic granulites of the Ubendian Belt, (2) to establish the *P-T* conditions in order to get the depth of equilibration of the mafic granulites and a possible *P-T* path, (3) perform major and trace elements systematics so as to be able to compare the composition of mafic granulites from the Ubendian Belt to granulites of other terranes elsewhere.

GEOLOGICAL SETTING

The Ubendian Belt extends for more than 500 km between the Tanzania Craton and the Bangweulu Block. It has been divided

into eight NW-SE oriented lithotectonic terranes, six of which are indicated in Fig.1. The terranes are internally deformed and are separated by extensive tracts of mylonitic and ultra-mylonitic gneisses (Daly *et al.* 1985, Daly 1988). These terranes (dominant lithologies in brackets) are: Ubende (hornblende gneisses), Wakole (aluminosilicate schists), Katuma (migmatitic biotite gneisses), Ufipa (granitic gneisses), Mbozi (metabasites), Lupa (meta-volcanics), Upangwa (meta-anorthosite), Nyika (cordierite gneisses).

Mafic granulites crop out in all of the Ubendian Belt terranes. Mafic granulite bodies, at several meter scales and in most cases forming elevated land, are tectonically emplaced and interlayered with other high-grade rocks e.g. garnet-biotite gneisses, augen gneisses, biotite-pyroxene gneisses. Sampled mafic granulites from the terranes of Katuma, Ufipa and Mbozi are massive and commonly with equant fine to medium grains of clinopyroxene-orthopyroxene-garnet-plagioclase \pm quartz. Garnet occurs as corona between plagioclase and pyroxenes.

Ring *et al.* (1997) considered the term Ubendian-Usagaran Orogeny to encompass active plate-margin process during a Paleoproterozoic orogenic cycle at the eastern and southern margin of the Archean Tanzania Craton. The granitic intrusion or metamorphic rocks with ages between 2100-1900 Ma are defined to have formed in the Ubendian-Usagaran Orogenic cycle. Comprehensive works by Lenoir *et al.* (1994) and Ring *et al.* (1997) have uncovered the crystallization age of volcanic-arc related granitoid-magmatism of the Ubendian Belt at ca. 2080-1850 Ma. Consequently, based on geochronological and geochemical data of granitoids Ring *et al.* (1997) proposed a long-lived Andean-type Paleoproterozoic subduction zone in the Ubendian Belt. The complex nature of the Ubendian Belt is further shown in the work of Boniface (2009), in which it is demonstrated that the Ubendian Belt has

been subjected to three different tectonic events (orogenic cycles) since its formation; first the Palaeoproterozoic (Eburnian) ocean-floor subduction at ca. 1890-1860 Ma and collision event at ca. 1830 Ma, followed by the Mesoproterozoic (Kibaran) crustal thickening and granulite-facies mylonitic reworking of the Palaeoproterozoic rocks at 1170-1010 Ma and lastly the Neoproterozoic (Pan-African) eclogite-facies metamorphism of small-ocean floor basalts and high-grade up to granulite-facies reworking at ca. 590-540 Ma of the Palaeoproterozoic precursors.

MATERIALS AND METHODS

A total of 9 samples were collected from the terranes of Ufipa, Mbozi, and Katuma (Fig. 1). Samples T126-1-04, T74-1-04, T36-1-06 and T12-1-06 were used for petrographic studies in order to establish P-T conditions. Geochemical investigations were performed on samples T71-2-04, T73-1-04, T81-1-04, T85-1-04 and T92-1-04. One sample (T73-1-04) was used for SHRIMP dating.

Minerals on thin sections were analysed using a 'JEOL Superprobe JXA-8900R' electron microprobe at the University of Kiel. For quantitative analyses the acceleration potential used for analyses was 15 to 20 kV for a beam current of 20 nA. The raw data were corrected by using the CITZAF method (Armstrong 1995).

Major and trace element concentrations of whole rocks were analyzed at the University of Kiel. A Philips PW 1400 X-ray fluorescence analyzer was used to acquire major element concentrations on fused glass discs, which were prepared by mixing in a platinum crucible 0.6 g of sample powder with 3.6 g of $\text{Li}_2\text{B}_4\text{O}_7$. The mixture was then subjected to the OXIFLUX 5-stage burner. Trace elements were measured using the Agilent 75000C ICP-MS instrument, using a sample preparation procedure described by Garbe-Schönberg (1993) and John *et al.* (2008). Analyzing international reference materials (BHVO-2 referer to

Table 4), blanks and some sample duplicates ensured data quality, precision and accuracy.

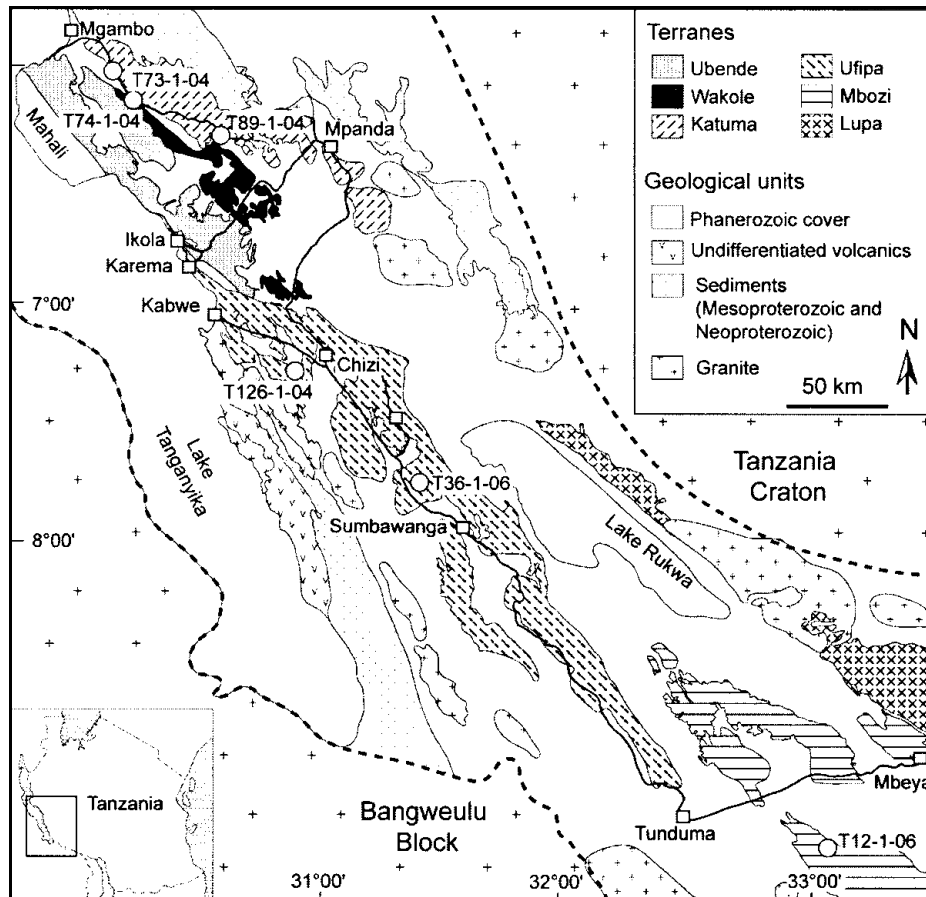


Figure 1: Geological map of the Ubendian Belt showing sample localities of mafic granulites. Map drawn after published quarter degree sheet maps of Smirnov *et al.* (1973).

Zircons were separated from crushed rocks using conventional magnetic and heavy liquid methods at the University of Kiel. Isotopic *U-Pb* dating of zircon was performed on a SHRIMP-II at the Center of Isotopic Research of VSEGEI in St. Petersburg, Russia. Handpicked round and prismatic zircons were mounted in epoxy resin discs and polished to expose their cores, and then were photographed in transmitted light and imaged using cathodoluminescence (CL). The diameter of the ion beam was approximately 20 μm and the primary beam intensity was about 4 nA.

Data reduction was done in the manner described by Williams (1998), using the SQUID Excel Makro by Ludwig (2001). Pb/U ratios have been normalized relative to a value of 0.0668 for the $^{206}\text{Pb}/^{238}\text{U}$ ratio of the TEMORA-1 internal standard reference zircon, equivalent to an age of 416.75 Ma (Black *et al.* 2003).

RESULTS

Petrography and mineral chemistry

Orthopyroxene, clinopyroxene, garnet, hornblende, plagioclase and quartz is a frequent mineral assemblage for the mafic

granulites of the Ubendian Belt (Fig. 2). High-pressure granulites without orthopyroxene were also sampled (Fig. 2A). The assemblage orthopyroxene, clinopyroxene, garnet with small amount or

without quartz and plagioclase has also been observed in some rocks. One sample (T126-1-04) from the Ufipa terrane is silica undersaturated and contains corundum instead of quartz (Fig. 2C).

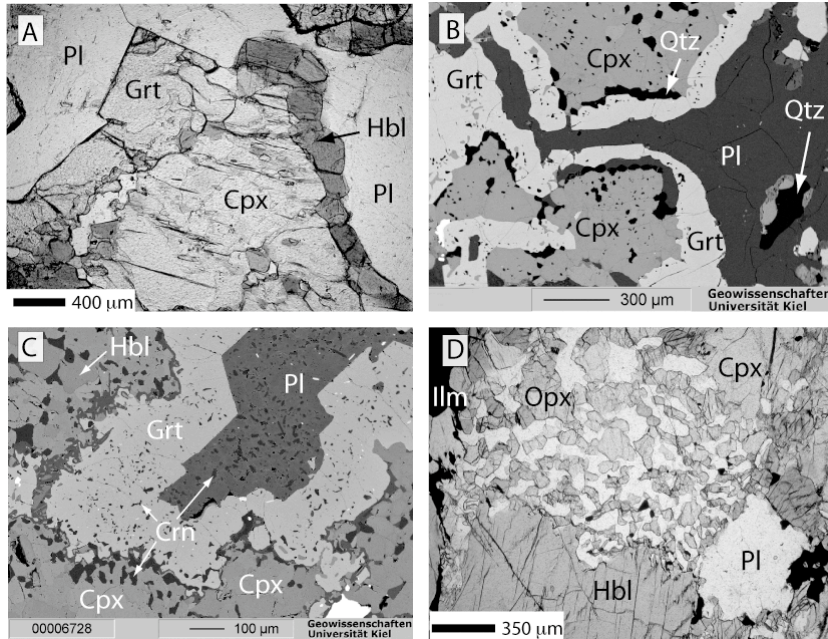


Figure 2: Mineral textures in mafic granulites of the Ubendian Belt. A&B: Garnet corona between clinopyroxene and Plagioclase. C: Corundum needles enclosed in plagioclase, garnet corona, and clinopyroxene. D: Orthopyroxene-clinopyroxene symplectites and the margins of hornblende.

Garnet corona between clinopyroxene and plagioclase is a characteristic feature for most of the sampled mafic granulites of the Ubendian Belt. Garnet coronas in granulites are traditionally interpreted as textures that form during isobaric cooling of granulite terranes (Bohlen 1987, Harley 1989, Spear 1993). Symplectites of orthopyroxene, clinopyroxene, ilmenite and plagioclase around hornblende were observed in some mafic granulite samples from the Mbozi terrane (Fig. 2D). This reaction texture has been reported from other world's granulite terranes (Schreyer 1983, Schenk 1984), in which it was interpreted as a result of temperature rise at constant pressure.

Garnet corona has a width of up to 0.5 mm. It is Fe-Mg rich with X_{Fe} (Fe/(Fe+Mg)) ranging between 0.50 and 0.64 (Table 1). X_{Grs} of about 0.21 in garnet corona of the high-pressure granulite (sample T12-3-06) is slightly higher when compared to that of orthopyroxene granulites of about 0.17-0.18 in other samples. The representative garnet composition in sample T126-1-04 is: $X_{Alm}=0.40$, $X_{Psp}=0.40$, $X_{Grs}=0.18$ and $X_{Sps}=0.01$.

Plagioclase of different samples have a wide range of composition with $X_{An}=0.25-0.78$, however the majority of samples have X_{An} ranging from 0.25 to 0.36 (Table 1).

Table 1: Representative composition of garnet and plagioclase.

	T126-1-04	T36-1-04	T12-3-06	T74-1-04		T126-1-04	T12-3-04	T74-2-04	T2-3-06
No.	86	102	20	190		91	37	236	137
Garnet					Plagioclase				
SiO ₂	39.63	39.44	38.76	39.28	SiO ₂	60.46	58.23	58.78	48.74
Al ₂ O ₃	23.02	21.55	22.34	21.72	Al ₂ O ₃	24.61	26.38	25.86	32.54
FeO	19.50	21.68	23.19	24.50	Fe ₂ O ₃	0.19	0.13	0.12	0.10
MgO	10.88	9.60	7.34	7.60	CaO	5.72	7.75	7.96	15.45
CaO	6.79	6.40	7.84	6.19	Na ₂ O	7.68	6.74	6.78	2.53
MnO	0.48	1.00	0.64	0.80	K ₂ O	0.37	0.10	0.44	0.08
Cr ₂ O ₃	0.00	0.35	0.00	0.00	Total	99.03	99.34	100.03	99.50
Total	100.30	100.22	100.11	100.09					
Cation: 12 oxygen					Cation: 8 oxygen				
Si	2.968	2.998	2.974	3.019	Si	2.711	2.615	2.630	2.238
Al	2.032	1.934	2.021	1.968	Al	1.301	1.397	1.363	1.762
Fe	1.221	1.378	1.488	1.575	Fe	0.007	0.005	0.004	0.004
Mg	1.215	1.088	0.839	0.871	Ca	0.275	0.373	0.381	0.762
Ca	0.545	0.520	0.644	0.052	Na	0.668	0.587	0.588	0.225
Mn	0.031	0.068	0.041	0.510	K	0.021	0.000	0.025	0.004
Cr	0.000	0.024	0.000	0.000	Total	4.983	4.983	4.993	4.990
Total	8.012	8.010	8.007	7.995					
X _{Fe}	0.501	0.555	0.639	0.644	X _{Ab}	0.693	0.608	0.591	0.227
X _{Alm}	0.405	0.450	0.494	0.524	X _{An}	0.285	0.380	0.383	0.768
X _{Prp}	0.403	0.350	0.279	0.290	X _{Or}	0.022	0.000	0.025	0.004
X _{Grs}	0.181	0.172	0.214	0.170					
G140	0.010	0.022	0.014	0.017					

Orthopyroxene is abundant in all samples except in sample T12-3-06 (high-pressure granulite). It occurs as a matrix or as a symplectite mineral. It is Mg rich with X_{Mg} (Mg/(Fe+Mg)) ranging between 0.64 and 0.73 (Table 2). No zoning profile was

observed for the analyzed matrix grains or symplectite. Compositions of matrix orthopyroxene and symplectites for sample T2-3-06 are similar (X_{Mg}=0.70 and Al₂O₃=2.5 wt%). Al₂O₃ composition in other samples range between 1.03 and 2.83

wt%. Clinopyroxene is a Mg rich diopside-augite with $X_{Mg}=0.70-0.84$ and contains low Na (Jd=0.5-13%; Table 2).

Table 2: Representative composition of clinopyroxene and orthopyroxene.

	T126-1-04	T36-1-06	T12-3-04	T74-1-04	T2-3-06	T36-1-04	T74-1-04	T2-3-06	T2-3-06
	101	95	45	218	120	77	215	67 _{Matrix}	23 _{Symplectite}
Clinopyroxene						Orthopyroxene			
SiO ₂	53.64	53.21	52.50	52.42	52.48	53.85	53.23	52.27	52.31
Al ₂ O ₃	3.84	1.44	2.76	2.09	2.78	1.71	1.26	2.87	2.27
TiO ₂	0.09	0.13	0.21	0.86	0.01	0.00	0.06	0.10	0.00
Cr ₂ O ₃	0.28	0.15	0.00	0.04	0.05	0.16	0.04	0.00	0.05
FeO	4.65	5.32	7.04	8.90	18.76	16.97	22.16	19.19	18.94
MgO	14.02	15.76	13.91	13.20	24.86	26.34	22.49	24.73	24.48
MnO	0.08	0.11	0.09	0.08	0.66	0.25	0.28	0.69	0.72
CaO	20.46	22.73	22.10	21.03	0.34	1.15	0.30	0.33	0.22
Na ₂ O	1.81	0.27	0.73	1.28	0.08	0.04	0.01	0.03	0.05
K ₂ O	0.02	0.03	0.01	0.01	0.00	0.00	0.02	0.00	0.00
Total	98.89	99.15	99.35	99.91	100.02	100.47	99.85	100.20	99.04
Cation: 12 oxygen									
Si	1.973	1.971	1.953	1.924	1.924	1.948	1.977	1.917	1.938
Al	0.167	0.063	0.121	0.090	0.120	0.073	0.055	0.124	0.099
Ti	0.003	0.004	0.006	0.024	0.000	0.000	0.002	0.003	0.000
Cr	0.008	0.005	0.000	0.001	0.001	0.005	0.001	0.000	0.001
Fe	0.143	0.165	0.219	0.246	0.575	0.513	0.688	0.589	0.587
Mg	0.769	0.870	0.771	0.722	1.358	1.421	1.245	1.352	1.352
Mn	0.002	0.003	0.003	0.003	0.021	0.008	0.009	0.021	0.023
Ca	0.807	0.902	0.881	0.827	0.013	0.045	0.000	0.013	0.009
Na	0.129	0.019	0.053	0.091	0.006	0.003	0.001	0.002	0.004
K	0.001	0.002	0.001	0.000	0.000	0.000	0.008	0.000	0.000
Total	4.002	4.002	4.007	3.929	4.018	4.015	3.986	4.020	4.013
Jd%	13	2.1	5.3	3.7	0.5				
X_{Mg}	0.84	0.84	0.78	0.75	0.70	0.73	0.64	0.70	0.70

Retrograde corona of brown hornblende occurs at the margins of pyroxenes (Fig. 2A), it has extremely low TiO₂, FeO and MgO (<0.1 wt% per each oxide). Green hornblende with composition of edenite-pargasite occurs as prograde relicts, partly dehydrated to form symplectites of orthopyroxene, clinopyroxene, and ilmenite (Fig. 2D).

P-T conditions

A summary of *P-T* conditions for the mafic granulites of the Ubendian Belt is given in Table 3 and plotted in Figure 3. Geothermometers that use Fe-Mg exchange between garnet and clinopyroxene as calibrated by Ellis and Green (1979), and Powell (1985) were used and yield

temperatures between 650 °C and 740 °C. The net-transfer equilibria (garnet, clinopyroxene, plagioclase, and quartz) geobarometers as calibrated by Newton and Perkins (1982), Powell and Holland (1988) and a garnet-orthopyroxene equilibria geobarometer as calibrated by Harley (1985) yield a pressure range between 7 kbar and 10.5 kbar. The pressure and temperature values obtained from the mafic granulites of the Ubendian Belt point to a geothermogradient of 22-28 °C/km in the lower crustal levels at a depth of 23-33 km. Isobaric cooling as suggested by garnet and hornblende coronas between clinopyroxene and plagioclase imply a long stay of these rocks at lower crustal levels before they were exhumed.

Table 3: Results of pressure and temperature estimates of the mafic granulites. Geothermometers: Grt-Cpx: Fe-Mg exchange; EG=Ellis and Green (1979), P=Powell (1985). Grt-Pl-Cpx-Qz geobarometers: NP=Newton and Perkins (1982), PH=Powell and Holland (1988), and Grt-Opx equilibria geobarometer

Sample No.	Analyses as per table 1&2	Calibrations		T (°C)	P (kbar)	Mineral assemblage
		Geotherm.	Geobar.			
T12-1-06	Grt ₂₀ -Cpx ₄₅ -Pl ₃₇	EG, P	PH, NP	700	9	Grt-Cpx-Pl-[Hbl]-Qtz-Ilm
T36-1-06	Grt ₁₀₃ -Opx ₇₇ -Cpx ₉₅	EG, P	H	700	8	Grt-Opx-Cpx- Hbl -Pl
T74-1-04	Grt ₁₉₀ -Opx ₂₁₅ -Cpx ₂₁₈ -Pl ₂₃₆	EG, P	PH, NP	650	7	Grt-Opx-Cpx-Pl-[Hbl]-Qtz-Ilm
T126-1-06	Grt ₈₆ -Cpx ₁₀₁ -Pl ₉₁	EG, P	PH, NP	740	10.5	Grt-Cpx-Pl-[Hbl]-Qtz-Ilm-Crn-Apt

[Hbl] = retrograde hornblende; _Hbl_ = prograde hornblende; Geotherm.= Geothermometer

Geobar.= Geobarometer

Geochemistry

Major and trace element systematics were performed in order to establish the geochemical signature and therefore tectonic setting of the mafic granulites of the Ubendian Belt.

Five samples were selected for carrying out geochemical analyses of major and trace elements and the results are given in Table 4. SiO₂ composition ranges from 47.37 to

50.76 wt. % this points to mafic or basaltic compositions. The total alkali silica (TAS) diagram of Irvine and Baragar (1971) and Le Maitre (1989) for discriminating types of basalts is consistent with the Zr/Ti vs Nb/Y diagram of Winchester and Floyd (1977) and Pearce (1996) despite the mobility of Na₂O and K₂O during metamorphism (e.g. Tatsumi *et al.* 1986). The samples plot as tholeiite basalts in both diagrams (Fig. 4A&B).

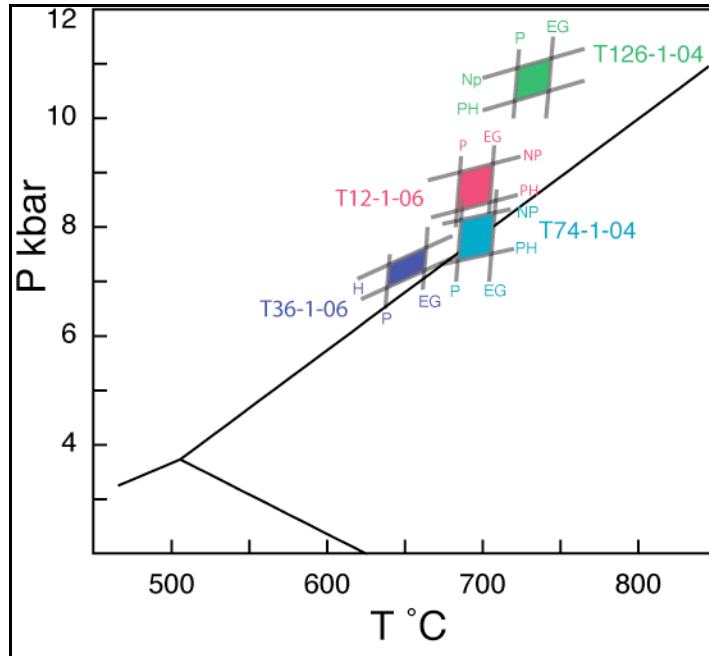


Figure 3: *P-T* conditions in the mafic granulites of the Ubendian Belt. Geothermometers: EG=Ellis and Green (1979), P=Powell (1985). Geobarometers: NP=Newton and Perkins (1982), PH=Powell and Holland (1988), H=Harley (1985).

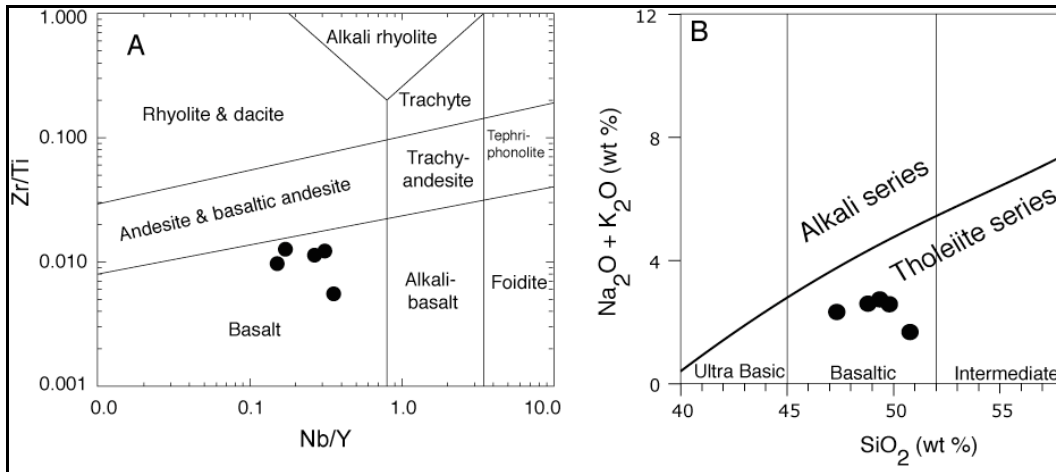


Figure 4: Magma discrimination diagrams showing the composition of mafic granulites of the Ubendian Belt. All samples plot in the field of tholeiite basalt magma in both plots A: Zr/Ti vs Nb/Y diagram of Pearce (1996) and B: Total alkali silica (TAS; Irvine and Baragar 1971, Le Maitre, 1989).

Table 4: Major and trace element composition of the mafic granulites of the Ubendian Belt

Sample	T71-2-04	T73-1-04	T81-1-04	T85-1-04	T92-1-04	BHVO-2 literature	BHVO-2	BHVO-2 Duplicate	Diff. %
Major elements (wt%)									
SiO ₂	50.76	49.84	49.46	47.37	48.81	49.88	49.96	50.01	0.1
TiO ₂	0.54	1.69	1.33	2.70	2.03	2.79	2.78	2.78	0.0
Al ₂ O ₃	13.89	13.16	13.19	12.35	12.39	13.63	13.54	13.53	-0.1
Fe ₂ O ₃	9.25	15.99	15.40	18.13	16.42	12.16	12.14	12.13	-0.1
MnO	0.17	0.23	0.24	0.24	0.23	0.17	0.17	0.17	0.0
MgO	10.03	5.53	6.16	6.02	5.44	6.98	6.93	7.07	2.6
CaO	13.79	10.34	10.75	10.58	10.08	11.56	11.56	11.51	-0.4
Na ₂ O	1.42	2.25	2.44	1.83	2.06	2.62	2.62	2.59	-1.1
K ₂ O	0.27	0.33	0.29	0.49	0.53	0.53	0.53	0.53	0.0
P ₂ O ₅	0.06	0.15	0.11	0.38	0.19	0.28	0.28	0.28	0.0
LOI	0.00	0.00	0.00	0.31	1.47	0.00	0.00	0.00	
Total	100.18	99.51	99.37	100.40	99.65	100.60	100.51	100.60	
Trace elements (ppm)									
Li	4.74	10.85	18.80	8.34	11.23	4.58	4.36	4.49	-3.6
Sc	54.5	44.9	43.5	50.4	50.8	33.0	31.6	30.2	4.5
V	259	397	303	357	359	332	321	302	6.6
Cr	240	23	27	75	63	363	363	363	0.0
Co	52.7	56.0	57.8	54.5	53.0	46.3	45.0	43.0	4.5
Ni	167	52	61	53	68	124	121	115	5.6
Cu	76.9	104	152	49	303	136	132	127	3.9
Zn	57.5	129	96	126	173	112	111	105	5.5
Ga	13.6	19.8	16.9	16.9	19.6	22.5	22.7	21.9	3.3
Rb	7.48	9.43	12.5	13.5	20.6	9.39	9.43	8.96	5.6
Sr	174	177	164	136	160	405	406	385	5.2
Y	14.4	28.2	22.7	28.0	37.9	26.3	26.5	25.6	3.5
Zr	40.3	113.6	76.4	89.3	147	177	176	166	5.7
Nb	2.47	7.50	3.44	9.96	11.8	17.8	16.7	16.9	-1.4
Cs	0.155	0.067	0.127	0.537	1.08	0.102	0.101	0.097	4.6
Ba	124	83	88	216	152	137	132	130	2.1
La	5.57	9.26	5.35	14.9	14.3	15.1	14.9	14.6	2.6
Ce	11.7	22.3	13.1	31.6	33.1	37.2	36.7	35.5	3.1
Pr	1.56	3.31	2.07	4.23	4.65	5.29	5.20	5.07	2.4
Nd	6.69	15.1	10.4	18.3	20.5	24.2	23.9	23.3	2.3

Sm	1.68	4.14	3.17	4.42	5.28	5.97	5.94	5.80	2.3
Eu	0.614	1.32	1.16	1.59	1.53	2.03	2.00	1.96	2.3
Gd	1.97	4.50	3.91	4.99	5.78	6.26	6.16	5.98	2.9
Tb	0.349	0.773	0.674	0.839	1.00	0.928	0.919	0.898	2.3
Dy	2.21	4.66	4.33	5.40	6.15	5.26	5.17	5.09	1.5
Ho	0.466	0.949	0.896	1.14	1.28	0.965	0.950	0.935	1.6
Er	1.35	2.66	2.45	3.21	3.67	2.40	2.36	2.31	2.4
Tm	0.193	0.379	0.361	0.485	0.531	0.325	0.319	0.314	1.6
Yb	1.23	2.42	2.35	3.27	3.43	1.98	1.96	1.90	3.0
Lu	0.182	0.356	0.348	0.504	0.518	0.277	0.272	0.267	1.6
Hf	0.995	2.79	2.26	2.61	3.67	4.41	4.32	4.29	0.7
Ta	0.142	0.446	0.229	0.659	0.703	1.12	0.855	1.07	-25.5
Pb	2.34	4.19	2.80	4.33	13.17	1.55	1.71	1.56	9.1
Th	0.822	1.24	0.429	1.83	2.15	1.23	1.21	1.18	2.5
U	0.154	0.296	0.132	0.493	0.619	0.418	0.406	0.402	0.9

The chondrite-normalized rare earth element (REE) patterns of these granulite reveal an enrichment of the light rare earth elements (LREEs) in which they range at 18-50 times chondritic values and the heavy rare earth elements (HREEs) range at 6-16 times chondritic values (Fig. 5A). The negative Eu anomaly is missing in all samples except sample T92-1-04, which has a measure of $Eu/Eu^* = 0.9$ pointing to slightly negative Eu anomaly. The absence of negative Eu anomaly may be attributed to a very deep source of melt precursors in which plagioclase was absent during partial melting. Patterns of the REE and concentration levels in these granulites remarkably resemble and are comparable to that of the average lower continental crust (Rudnick and Gao 2003).

The MORB-normalized REE and high field strength elements (HFSE) patterns and concentrations reveal conspicuously similar features to that of average lower continental crust (Fig. 5B). Features like negative

anomaly of the HFSE (Nb-Ta, Hf-Zr) and enrichment of the alkali earth metals (Cs, Rb, Ba) resemble that of the lower continental crustal rocks.

Geochronology

Zircon Texture and Composition

Sub-rounded zircons were separated from sample T73-1-04 (mineral assemblage: garnet-orthopyroxene-clinopyroxene-plagioclase). Cathodoluminescent images reveal high-luminescent sector zoned cores partly covered by low-luminescent rims (Fig. 6). Compositionally U content ranges at 222-343 ppm and Th at 107-138 ppm in zircon cores and result into a Th/U ratio range at 0.39-0.57. The rims have U content ranging at 357-822 ppm and Th at 88-185 ppm, which result to the Th/U of 0.22-0.30 (Table 5). Absence of concentric growth zoning in these zircons and low Th/U may indicate growth of both cores and rims during metamorphism (Rubatto 2002, Corfu *et al.* 2003, Hoskin and Schaltegger 2003).

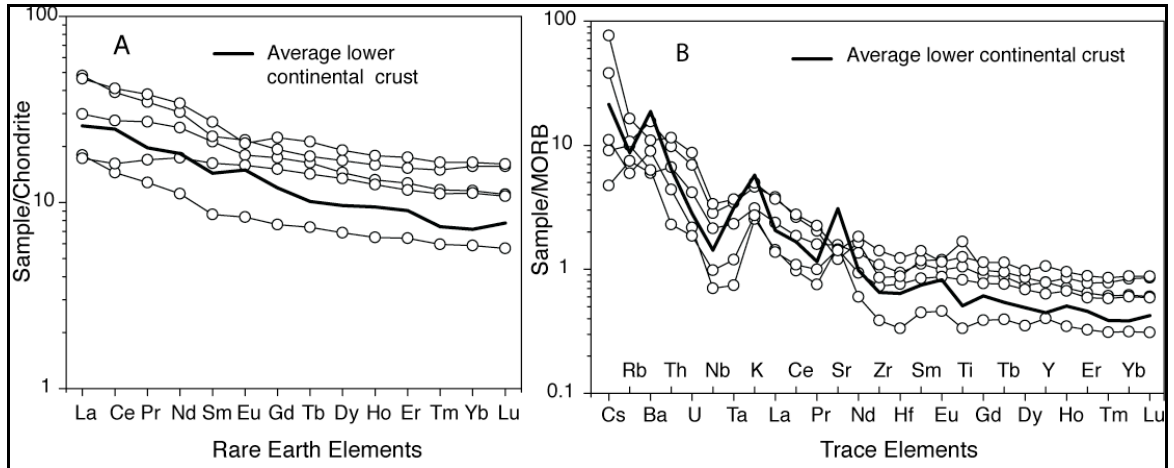


Figure 5: A: Chondrite-normalized REE concentrations of the Mafic granulite, the normalization values are from Boynton (1984) and the average composition of the lower crust are from Rudnick and Gao (2003). B: MORB-normalized trace element patterns; normalizing values after Hofmann (1988).

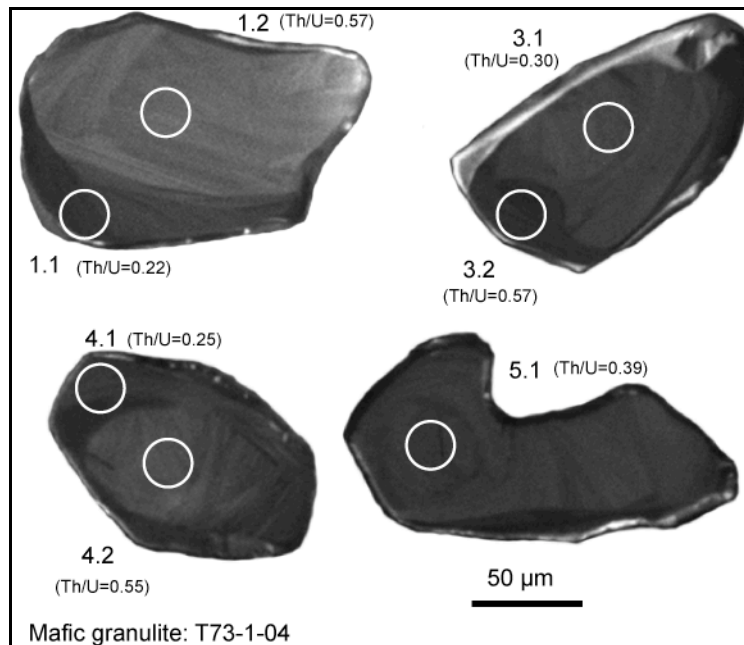


Figure 6: Cathodoluminescent images show subrounded zircons with high luminescent sector zoned cores partly covered by low-luminescent rims; there is no oscillatory or magmatic growth zones were observed. Zircon rims have relatively lower Th/U ratios in their rims than the surrounded cores.

Table 5: SHRIMP U-Pb zircon composition of the mafic granulites of the Ubendian Belt.

Spot	U (ppm)	Th (ppm)	Th/U	²³² Th/ ²³⁸ U	²⁰⁶ Pb* (%)	Apparent age (Ma)		²⁰⁷ Pb/ ²⁰⁶ Pb ±	²⁰⁶ Pb/ ²³⁸ U ±	²⁰⁷ Pb*/ ²⁰⁶ Pb ±(%)	error ±(%)	²⁰⁶ Pb*/ ²³⁸ U ±(%)	²⁰⁷ Pb*/ ²³⁵ U ±(%)	error (%)	Disc. (%)	
						²⁰⁷ Pb/ ²⁰⁶ Pb	²⁰⁶ Pb/ ²³⁸ U									
rims																
1.1	822	185	0.22	0.23	0.17	1942	10	1909	10	0.12	0.55	0.34	0.62	5.657	0.83	2
3.1	407	124	0.30	0.31	0.03	1875	12	1800	10	0.11	0.66	0.32	0.65	5.105	0.93	4
4.1	357	88	0.25	0.26	0.12	1876	21	1883	11	0.11	1.20	0.34	0.69	5.368	1.4	0
cores																
1.2	242	137	0.57	0.58	0.08	1962	15	1918	13	0.12	0.85	0.35	0.78	5.752	1.2	2
3.2	222	107	0.48	0.50	0.26	1936	19	1887	13	0.12	1.10	0.34	0.79	5.564	1.3	3
4.2	253	138	0.55	0.56	--	1948	13	1944	12	0.12	0.75	0.35	0.74	5.799	1.1	0
5.1	343	134	0.35	0.40	0.09	1952	13	1923	11	0.12	0.74	0.35	0.69	5.737	1	1

*Common Pb corrected using measured ²⁰⁴Pb, errors are 1-sigma.

Ages

Seven points analyzed from cores and rims of four zircon grains are slightly discordant with an upper intercept plotting at 1977±40 Ma and a lower intercept at 1206±340 Ma (Fig. 7). The upper intercept date is here interpreted as the age of granulite-facies

metamorphism in the Ubendian Belt. The lower intercept date is not precisely defined, it was calculated with a huge error. However, this age clearly points out that in the Mesoproterozoic there was a metamorphic event in the Ubendian Belt that caused isotopic disturbance in zircons.

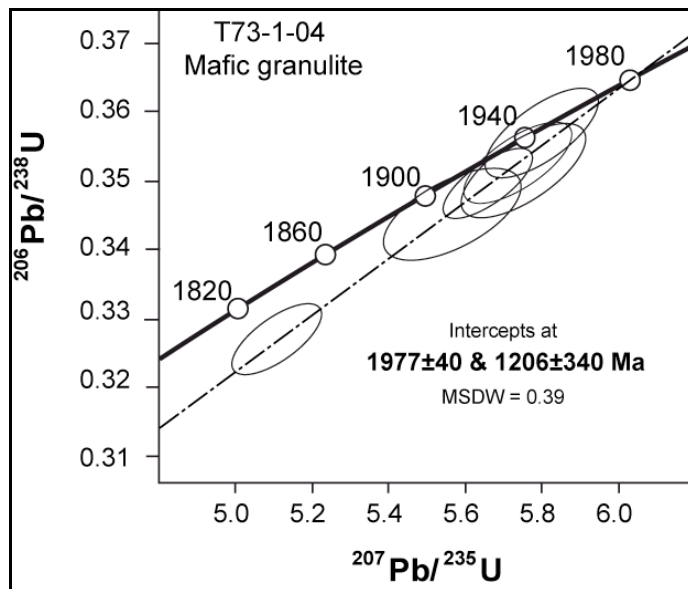


Figure 7: U-Pb Concordia diagram of zircons from Sample T73-2-04. A discordia yields an upper intercept Paleoproterozoic age at 1977±40 (error is given at 2s) and un-precise lower intercept Mesoproterozoic age

Precise ages of the Kibaran event between that occurred 1170 Ma and 1010 Ma in the Ubendian Belt is demonstrated in Boniface (2009). The above lower intercept date in the mafic granulite of sample T74-1-04 clearly indicates the Mesoproterozoic U-Pb isotopic disturbance in zircon. Probably the Mesoproterozoic orogenic event contributed to the process of exhuming the Paleoproterozoic lower crust mafic granulite, which resided at deep crustal level long enough to acquire isobaric cooling texture.

DISCUSSION AND CONCLUSIONS

Geochemical, petrological, and geochronological data indicate that mafic granulite of the Ubendian Belt belong to the Paleoproterozoic, 1977±40 Ma old, lower continental crust. These rocks have a typical geochemical signature of the average lower continental crustal basaltic rocks. Trace and REE patterns are similar to that published by Rudnick and Gao (2003) for the average lower continental crustal composition. These mafic granulite rocks of the Ubendian Belt resided at deep crustal levels between 23 and 33 km and stayed there for a long period of time, thus they geothermally relaxed and isobarically cooled. In the process of cooling garnet coronas developed between plagioclase and clinopyroxene, these two minerals reacted to each other. Possibly the Mesoproterozoic orogenic cycle contributed to the uplift of these lower crustal rocks.

Orthopyroxene, clinopyroxene, garnet, hornblende, plagioclase, and quartz is a frequent mineral assemblage for the mafic granulites of the Ubendian Belt. Geothermobarometry of the mafic granulites of the Ubendian Belt have revealed the equilibration of these rocks at temperatures between 650 °C and 740 °C and pressure between 7 kbar and 10.2 kbar equivalent to the geothermogradient of 22-28 °C/km and at a depth of 23-33 km.

Mineral assemblages in the mafic granulite samples of the Ubendian Belt do not assist

in deducing a complete path of *P-T* evolution. The retrograde isobaric cooling path is implied by garnet corona between plagioclase and clinopyroxene. The prograde path is masked by absence of prograde mineral assemblages. The thermal modals of Thompson and England (1984) demonstrate that rocks initially buried near the base of doubly thickened crust would re-equilibrate at shallower levels as amphibolites-granulites and would record no evidence of an earlier, lower grade history. Probably the mafic granulites of the Ubendian Belt were buried deeper than 33 km and re-equilibrated at shallower levels of the crust between 23-33 km.

The non-precise date at 1206±340 Ma indicates that following the Ubendian Orogenic cycle the orogenic cycle of the Mesoproterozoic (the Kibaran Orogeny) contributed to the exhumation of the deep crustal rocks of the Ubendian Belt. Precise dates of the Kibaran Orogenic cycle, which affected rocks of the Ubendian Belt have been established by Boniface (2009) and is between 1170 and 1010 Ma.

ACKNOWLEDGEMENTS

Thanks to DAAD and DFG (Sche 265/10) for funding this research. The help of V. Schenk during my stay in Kiel is very much appreciated. I wish to thank A. Mruma, T. John for their valuable supports in many forms. I thank the ICP-MS laboratory team under D. Garbe-Schönberg and his co-workers P. Fiedler and U. Westernströer for their assistance during sample preparation and analyses. Gratitude is due to B. Mader for her assistance handling samples with a microprobe and A. Fehler for producing high quality thin sections. I thank A. Larionov, I. Paderin, S. Presniakov and N. Rodionov, a team of the SHRIMP laboratory at St. Petersburg Russia for their cooperation and assistance in dating of zircons.

REFERENCES

- Armstrong JT 1995 CITZAF, a package of correction programs for the quantitative electron microbeam x-ray analysis of thick polished materials, thin films and particles. *Microbeam Analysis*. **4**: 117-200.
- Black LP, Kamo SL, Allen CM, Aleinikoff JN, Davis DW, Korsch RJ, Foudoulis C 2003 TEMORA 1, a new zircon standard for Phanerozoic U-Pb geochronology. *Chem. Geol.* **200**: 155-170.
- Bohlen SR 1987 Pressure-temperature-time paths and a tectonic model for the evolution of granulites. *J. Geol.* **95**: 617-632.
- Boniface N 2009 Eburnian, Kibaran and Pan-African metamorphic events in the Ubendian Belt (Tanzania): Petrology and zircon geochronology. Ph.D. thesis, University of Kiel, Germany.
- Boynton WV 1984 Cosmochemistry of the rare earth elements: meteorite studies. In: Handerson P (ed) *Rare earth element geochemistry*. Elsevier Sci. Publ. pp. 63-114.
- Corfu F, Hanchar JM, Hoskin PWO, Kinny PD 2003 Atlas of zircon textures. In: Zircon. Mineralogical Society of America and Geochemical Society, Washington, DC, United States. **53**: 469-500.
- Daly MC 1988 Crustal shear zones in central Africa: a kinematic approach to Proterozoic tectonics. *Episodes*. **11(1)**: 5-11.
- Daly MC, Klerkx J, Nanyaro JT, 1985 Early proterozoic terranes and strike-slip accretion in the Ubendian Belt of southwest Tanzania. *Terra Cognita (Abstract)* **5**: P257.
- Ellis DJ 1987 Origin and evolution of granulites in normal and thickened crusts. *Geology*. **15**: 167-170.
- Ellis DJ, Green DH 1979 An experimental study of the effect of Ca upon garnet-clinopyroxene Fe-Mg exchange equilibria. *Contributions to Mineralogy and Petrology*. **71(1)**: 13-22.
- Garbe-Schönberg CD 1993 Simultaneous determination of thirty-seven trace elements in twenty-eight international rock standards by ICP-MS. *Geostandards Newsletter* **17**.
- Harley LS 1985 An experimental study of the partitioning of Fe and Mg between garnet and orthopyroxene. *Contributions to Mineralogy and Petrology*. **86**: 359-373.
- Harley SL 1989 The origins of granulites: a metamorphic perspective. *Geological Magazine*. **126(3)**: 215-247.
- Hofmann AW 1988 Chemical differentiation of the earth: the relationship between mantle, continental crust, and oceanic crust. In: *Isotope geochemistry: the Crafoord symposium*. Elsevier, Amsterdam, Netherlands. **90 (3)**: 297-314.
- Hoskin PWO, Schaltegger U 2003 The composition of zircon and igneous and metamorphic petrogenesis. In: Zircon. Mineralogical Society of America and Geochemical Society, Washington, DC, United States. **53**: 27-62.
- Irvine TN, Baragar WRA 1971 A guide to the chemical classification of the common volcanic rocks. *Can. J. Earth Sci.* **8**: 523-548.
- John T, Klemd R, Gao J, Garbe-Schoenberg D 2008 Trace element mobilization in slabs due to non steady fluid-rock interaction: Constraints from an eclogite-facies transport vein in blueschist (Tianshang, China). *Lithos*. **103(1-2)**:1-24.
- Le Maitre RW 1989 A Classification of Igneous Rocks and Glossary of Terms: Recommendations of the International Union of Geological Sciences, Subcommittee on the Systematics of Igneous Rocks. Oxford: Blackwell.
- Lenoir JL, Liegeois JP, Theunissen K, Klerkx J 1994 The palaeoproterozoic Ubendian shear belt in Tanzania: geochronology and structure. *J. Afr. Earth Sci.* **19(3)**. 169-184.

- Ludwig K 2000 SQUID 1.02. A Users Manual. *Berkeley Geochronology Center Special Publication 2*, 19.
- Newton RC, Perkins DI 1982. Thermodynamic calibration of geobarometers based on the assemblages garnet-plagioclase-orthopyroxene (clinopyroxene)-quartz. *American Mineralogist*. **67(3-4)**: 203–222.
- Pearce JA 1996 A user's guide to basalt discrimination diagrams. In: Trace element geochemistry of volcanic rocks: applications for massive sulphide exploration. *Geological Association of Canada, John's, NF, Canada*. **12**: 79–113.
- Powell R 1985 Regression diagnostics and robust regression in geothermometer/geobarometer calibration: the garnet-clinopyroxene geothermometer revisited. *J. Metamorph. Geol.* **3(3)**: 231–243.
- Powell R, Holland TJB 1988 An internally consistent dataset with uncertainties and correlations: 3, applications to geobarometry, worked examples and a computer program. *J. Metamorph. Geol.* **6(2)**: 173–204.
- Ring U, Kroener A, Toulkeridis T, 1997 Palaeoproterozoic granulite-facies metamorphism and granitoid intrusions in the ubendian-usagaran orogen of northern Malawi, East-Central Africa. *Precamb. Res.* **85(1-2)**: 27–51.
- Rubatto D 2002 Zircon trace element geochemistry: partitioning with garnet and the link between u-pb ages and metamorphism. *Chem. Geol.* **184(1-2)**: 123–138.
- Rudnick LR, Gao S 2003 Composition of the continental crust. In: Rudnick, L. R. (Ed.), *The Crust. Treatise on Geochemistry*. Elsevier-Pergamon, Oxford. **3**: 1–64.
- Schenk V 1984 Petrology of felsic granulites, metapelites, metabasics, ultramafics, and metacarbonates from Southern Calabria (Italy): Prograde metamorphism, uplift and cooling of a former lower crust. *J. Petrol.* **25(1)**: 255–298.
- Schreyer W 1983 Metamorphism and fluid inclusions in the basement of the Vredefort Dome, South Africa: guidelines to the origin of the structure. *Journal of Petrology*. **24(1)**: 26–47.
- Smirnov V, Pentelkov V, Tolochko V, Trifan M, Zhukov S 1973 Geology and minerals of the central part of the western rift. Tech. rep., Mineral and Resource Division, Dodoma, Tanzania, unpublished report of the geological mapping.
- Spear FS, 1993 Metamorphic Phase Equilibria and Pressure-Temperature-Time Paths. Mineralogical Society of American MONOGRAPH. *Mineralogical Society of America, Washington, D.C., New York*. 799p
- Tatsumi Y, Hamilton DL, Nesbitt RW 1986 Chemical characteristics of fluid phase released from a subducted lithosphere and origin of arc magmas: evidence from high-pressure experiments and natural rocks. In: M. Sakuyama and H. Fukuyama memorial volume. Elsevier, Amsterdam, Netherlands. **29**: 293–309.
- Thompson AB, England PC 1984 Pressure-temperature-time paths of regional metamorphism II. their inference and interpretation using mineral assemblages in metamorphic rocks. *J. Petrol.* **25(4)**: 929–955.
- Whitney D, Evans BW 2010 Abbreviations for names of rock-forming minerals. *Am. Mineral.* **95**: 185–187.
- Williams I 1998 U-Th-Pb Geochronology by Ion Microprobe. In: McKibben, M., Shanks III, W., Ridley, W. (Eds.), *Application of microanalytical techniques to understanding mineralizing processes*. Reviews in Economic Geology. **7**:1–35.
- Winchester JA, Floyd PA, 1977 Geochemical discrimination of different magma series and their differentiation products using immobile elements. *Chem. Geol.* **20(4)**: 325–343.